Supplementary Materials

Sugarcane Bagasse Ash as a Catalyst Support for Facile and Highly Scalable Preparation of Magnetic Fenton Catalysts for Ultra-Highly Efficient Removal of Tetracycline

Natthanan Rattanachueskul [1], Oraya Dokkathin [1], Decha Dechtrirat [2,3,4], Joongjai Panpranot [5], Waralee Watcharin [6], Sulawan Kaowphong [7] and Laemthong Chuenchom [1,*]

[1] Division of Physical Science (Chemistry Program) and Center of Excellence for Innovation in Chemistry, Faculty of Science, Prince of Songkla University, Hat-Yai District, Songkhla 90110, Thailand; natthanan.rc@gmail.com (N.R.); orayamod.d@gmail.com (O.D.)
[2] Department of Materials Science, Faculty of Science, Kasetsart University, Bangkok 10900, Thailand; fscidcd@ku.ac.th
[3] Specialized Center of Rubber and Polymer Materials for Agriculture and Industry (RPM), Faculty of Science, Kasetsart University, Bangkok 10900, Thailand
[4] Laboratory of Organic Synthesis, Chulabhorn Research Institute, Bangkok 10210, Thailand
[5] Department of Chemical Engineering, Faculty of Engineering, Chulalongkorn University, Bangkok 10330, Thailand; joongjai.p@chula.ac.th
[6] Faculty of Biotechnology (Agro-Industry), Assumption University, Hua Mak Campus, Bangkok 10240, Thailand; waraleewtc0@gmail.com
[7] Department of Chemistry and Center of Excellence in Materials Science and Technology, Faculty of Science, Chiang Mai University, Chiang Mai 50200, Thailand; sulawank@gmail.com
* Correspondence: laemthong.c@psu.ac.th; Tel.: +66−74−288416; Fax: +66−74−558841

Citation: Rattanachueskul, N.; Dokkathin, O.; Dechtrirat, D.; Panpranot, J.; Watcharin, W.; Kaowphong, S.; Chuenchom, L. Sugarcane Bagasse Ash as a Catalyst Support for Facile and Highly Scalable Preparation of Magnetic Fenton Catalysts for Ultra-Highly Efficient Removal of Tetracycline. *Catalysts* **2022**, *12*, 446. https://doi.org/10.3390/catal12040446

Academic Editors: Sagadevan Suresh and Is Fatimah

Received: 14 March 2022
Accepted: 14 April 2022
Published: 18 April 2022

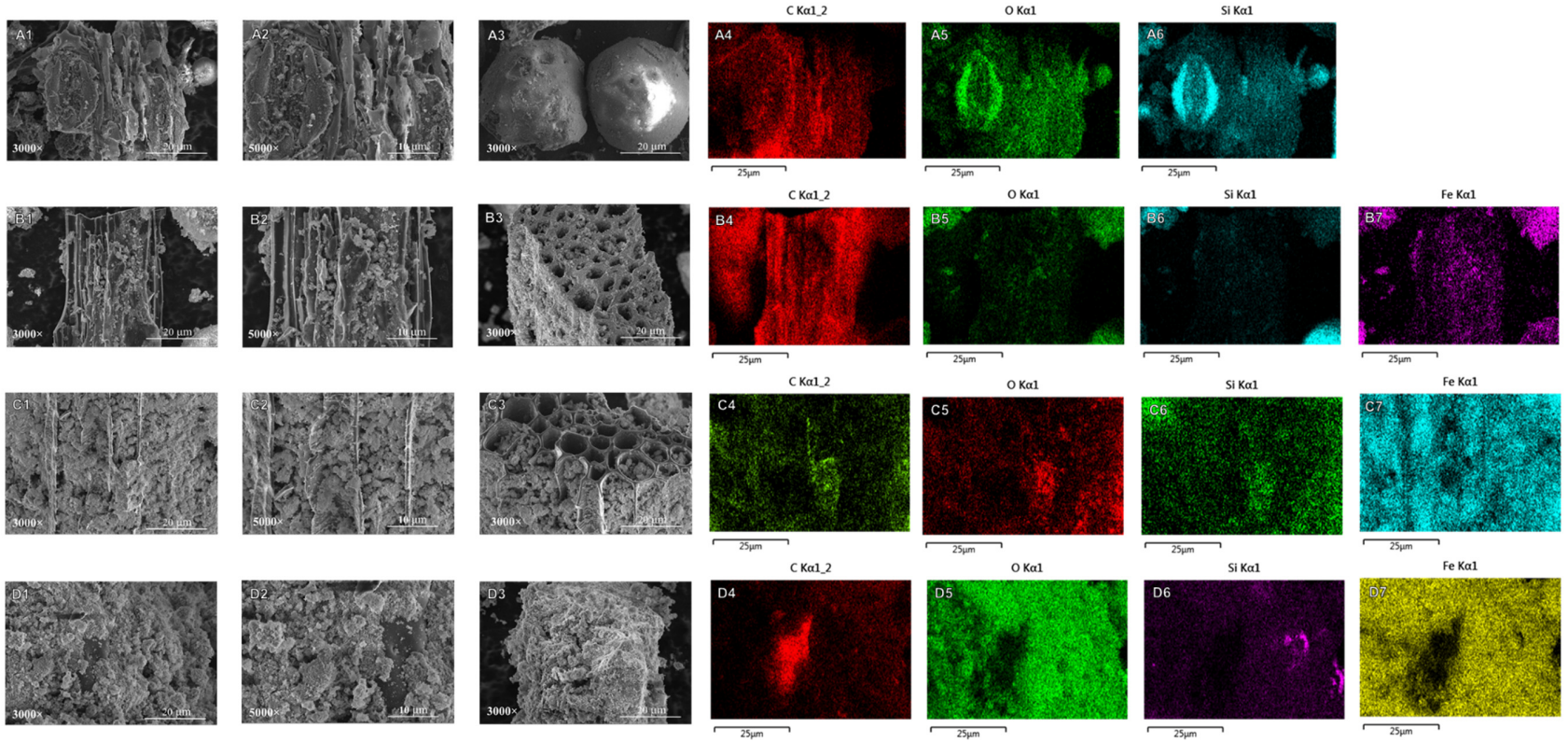

Figure S1. FESEM-EDX analysis. (A1-A3) FESEM images at 3000×-5000× of BGA, (A4-A6) Elemental mapping for C, O, and Si from (A1), (B1-B3) FESEM images at 3000×-5000× of MBGA2-1, (B4-B7) Elemental mapping for C, O, Si , and Fe from (B1), (C1-C3) FESEM images of MBGA2-1, (C4-C7) Elemental mapping for C, O, Si , and Fe from (C1), (D1-D3) FESEM images at 3000×-5000× MBGA2-2, and (D4-D7) Elemental mapping for C, O, Si , and Fe from (D1)

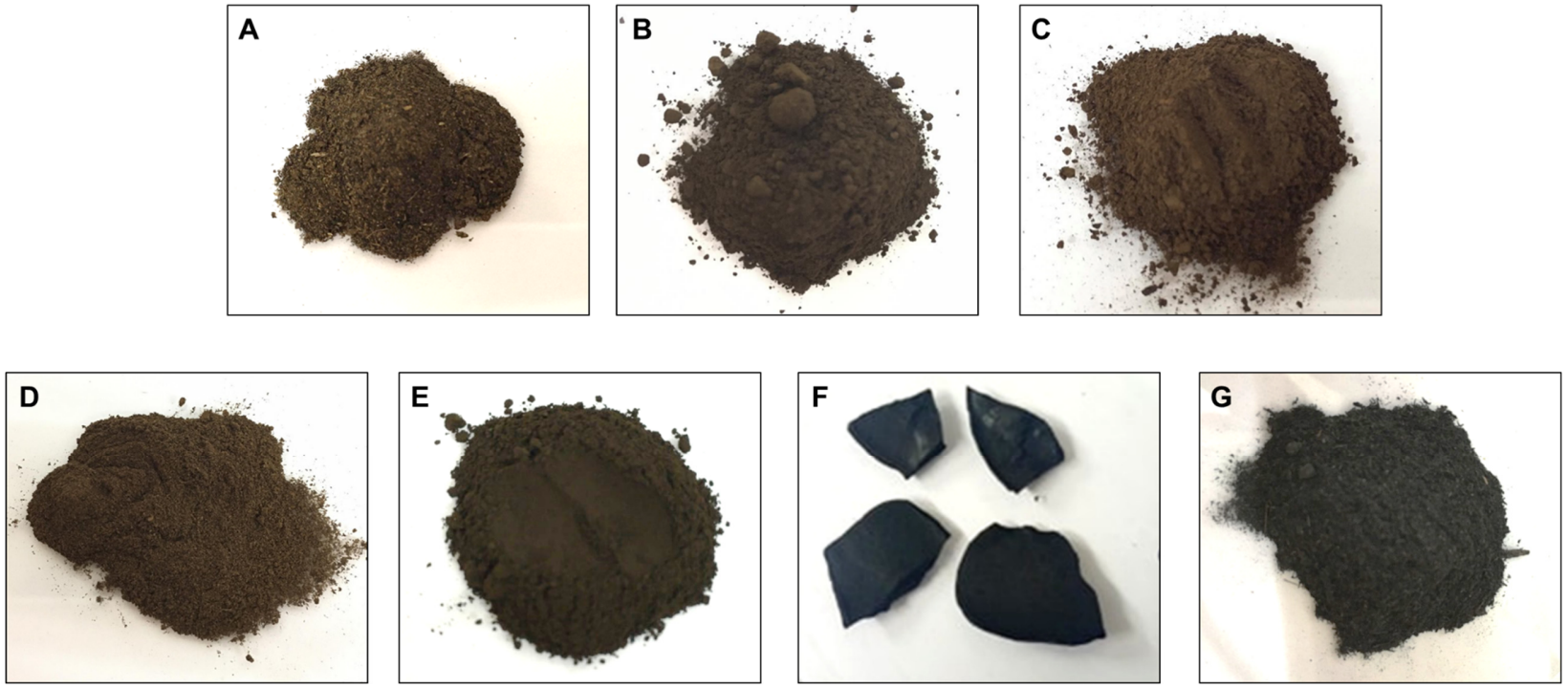

Figure S2. Physical images of A) MBGA1-1 b) MBGA2-1 C) MBGA5-1 D) MBGA2-0.5 E) MBGA2-2 F) Fe_3O_4 and G) BGA

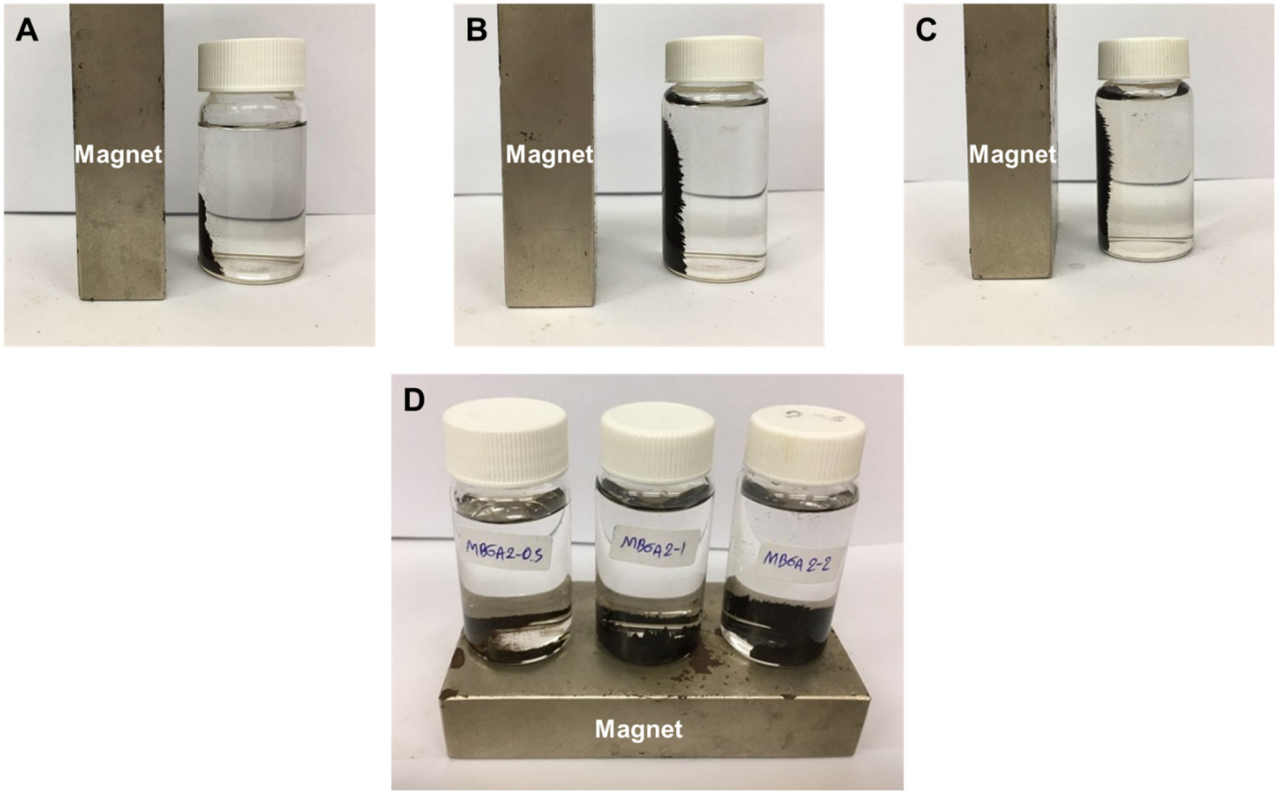

Figure S3. Physical image of magnetic separation of (A) MBGA2-0.5 (B) MBGA2-1 (C) MBGA2-2 from aqueous solution and (D) The magnetic sedimentation for MBGA samples

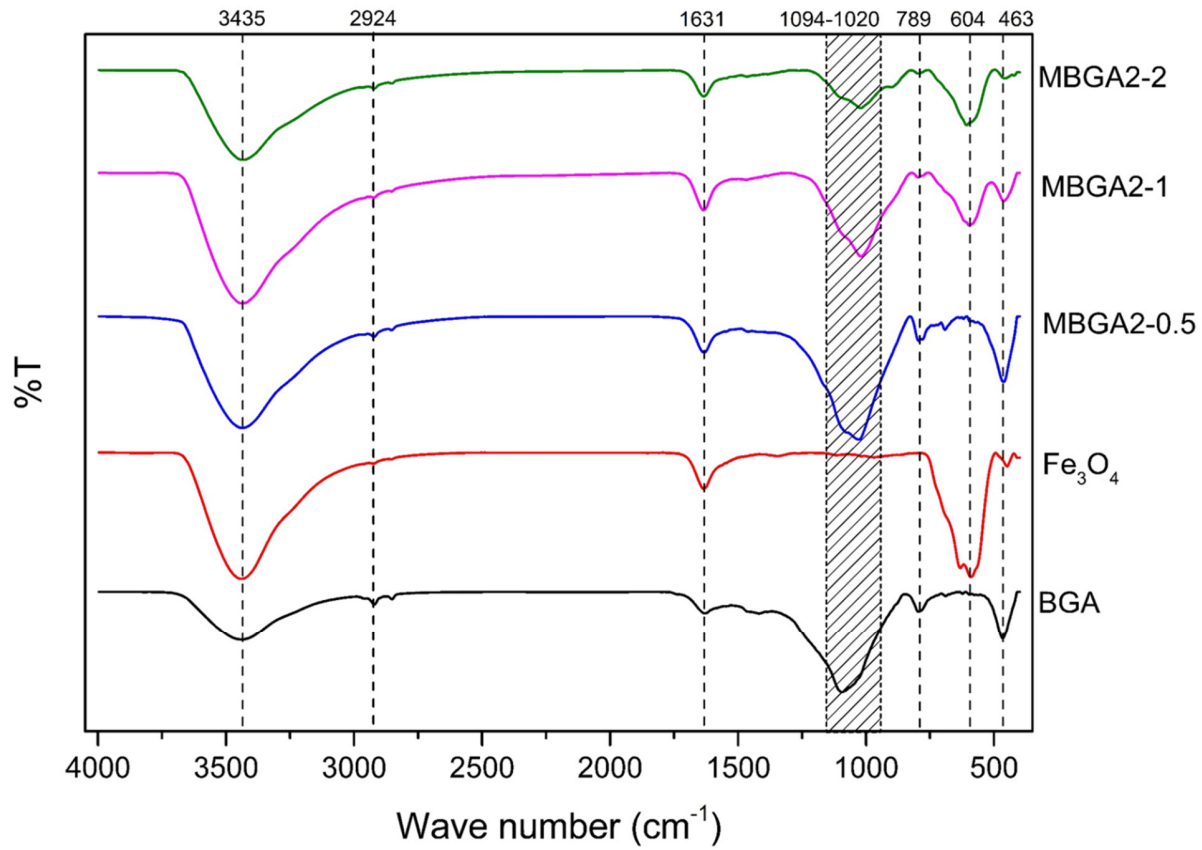

Figure S4. FTIR spectra for all samples

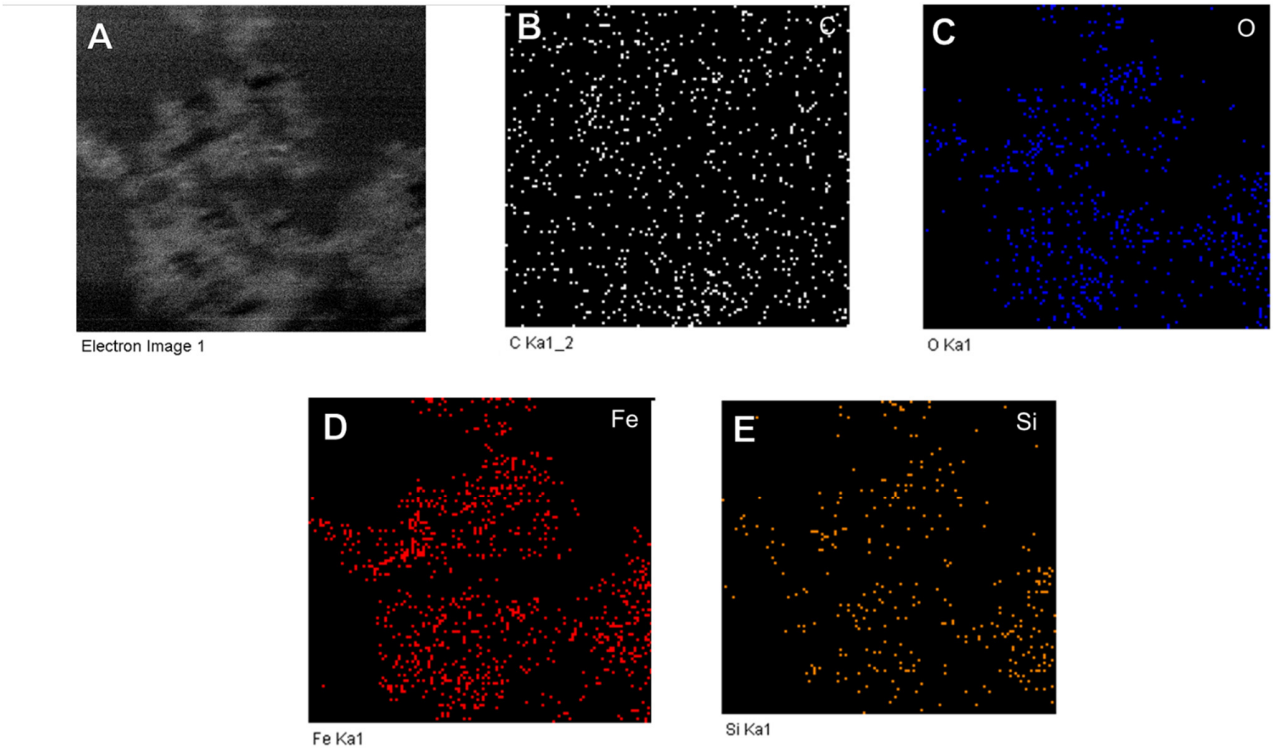

Figure S5. (A) TEM image in electron mode (B-E) EDS mapping of C, O, Fe, Si, respectively.

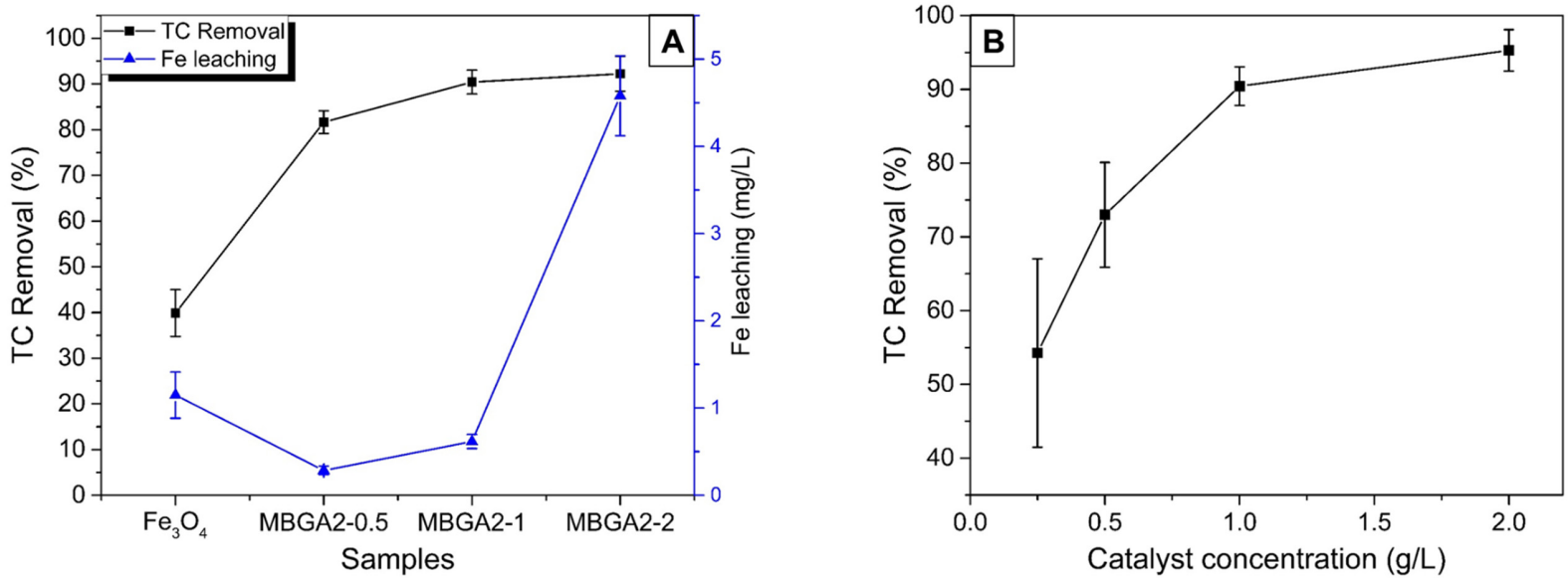

Figure S6. (A) Preliminary Catalytic Heterogeneous Fenton Reaction Test with Fe leaching for each samples, (B) The effect of catalyst concentration on the catalytic degradation of TC for MBGA2-1 (conditions: C_0 = 800 mg/L, pH 3.2 (natural), H_2O_2 concentration = 5 mM, catalyst concentration = 1 g/L , T = 28±2°C)

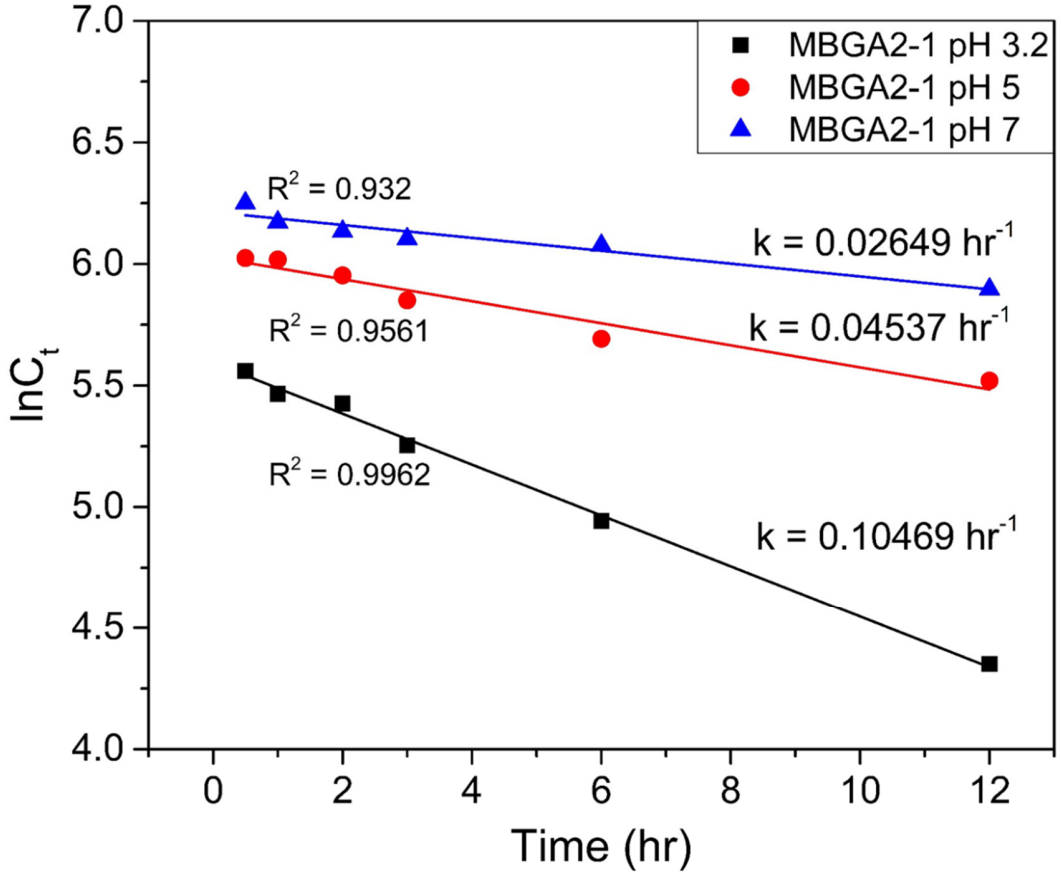

Figure S7. Linear pseudo-first-order kinetics model for the catalytic degradation of TC for MBGA2-1 under different pH

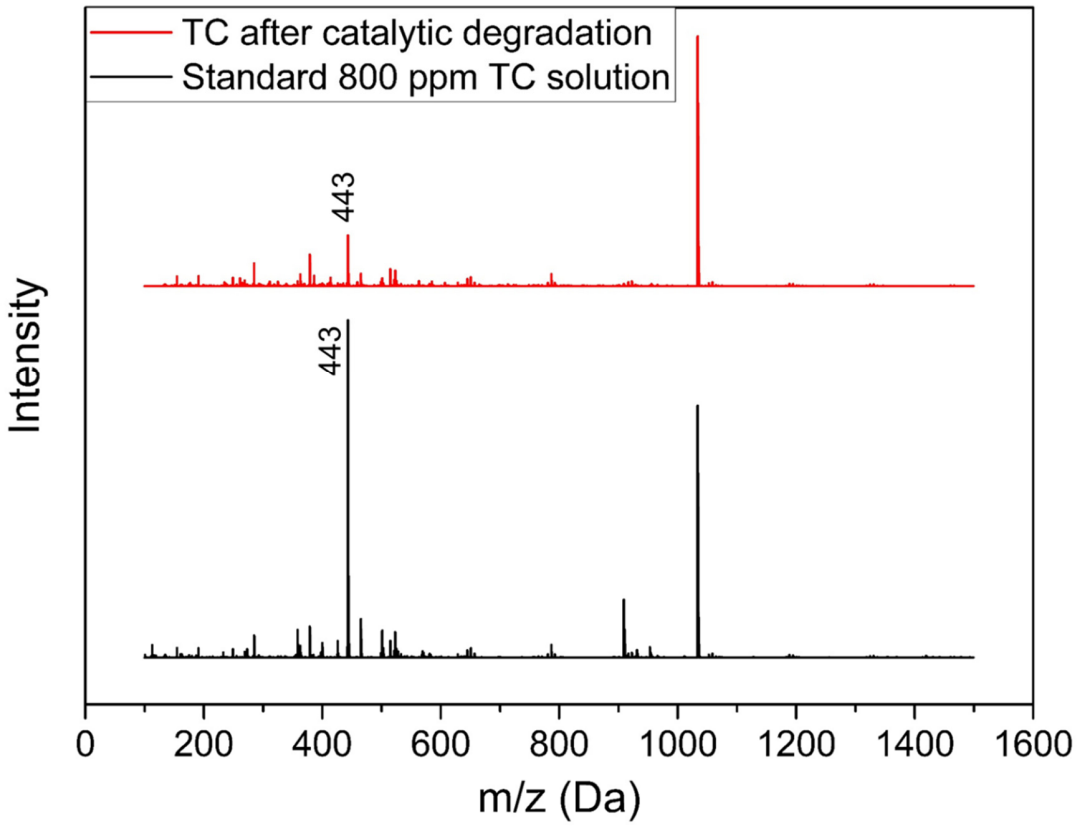

Figure S8. LC-MS of the TC solution before- and after- catalytic degradation by MBGA2-1

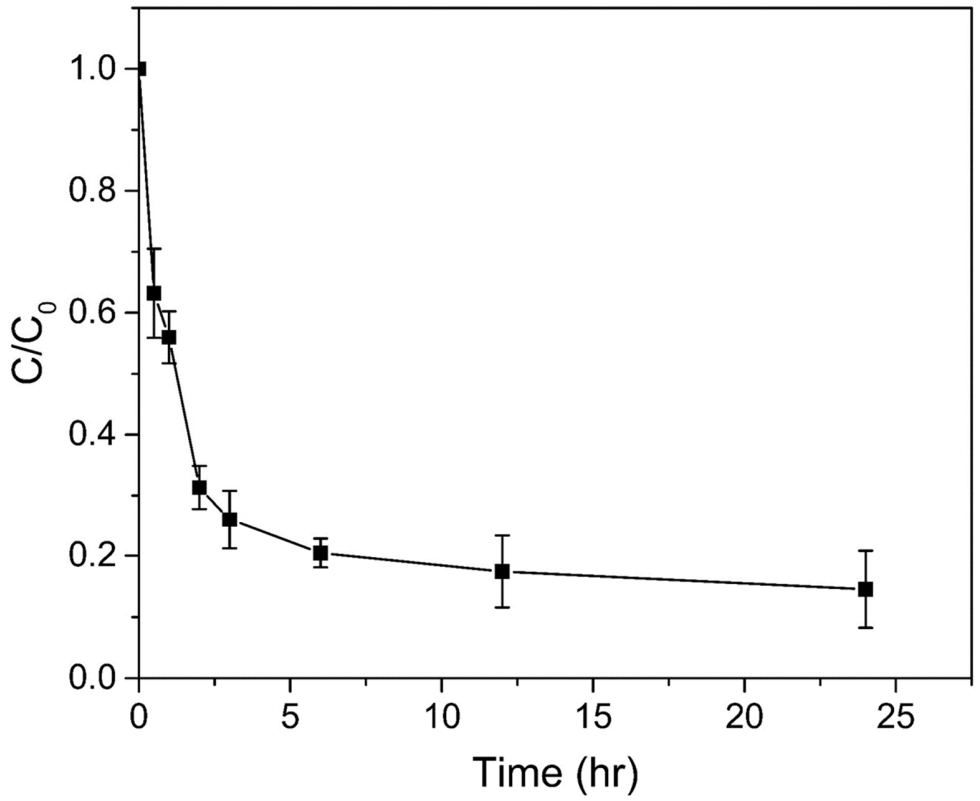

Figure S9. Comparative studies of the catalytic degradation of low concentration of TC for MBGA2-1 (conditions: C_0 = 40 mg/L, pH 3.2 (natural), H_2O_2 concentration = 5 mM, catalyst concentration = 1 g/L, T = 28±2°C)

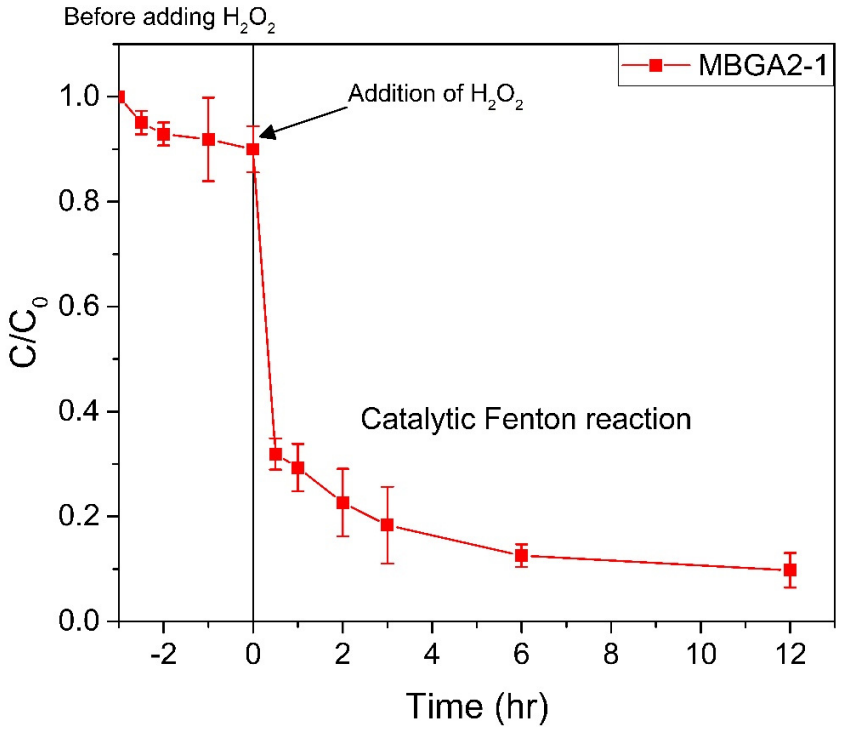

Figure S10. The catalytic degradation of TC for MBGA2-1. The Fenton reaction starting by the addition of H_2O_2 after the adsorption process in dark condition for 3 hr. (conditions: C_0 = 800 mg/L, pH 3.2 (natural), H_2O_2 concentration = 5 mM, catalyst concentration = 1 g/L, T = 28±2°C)

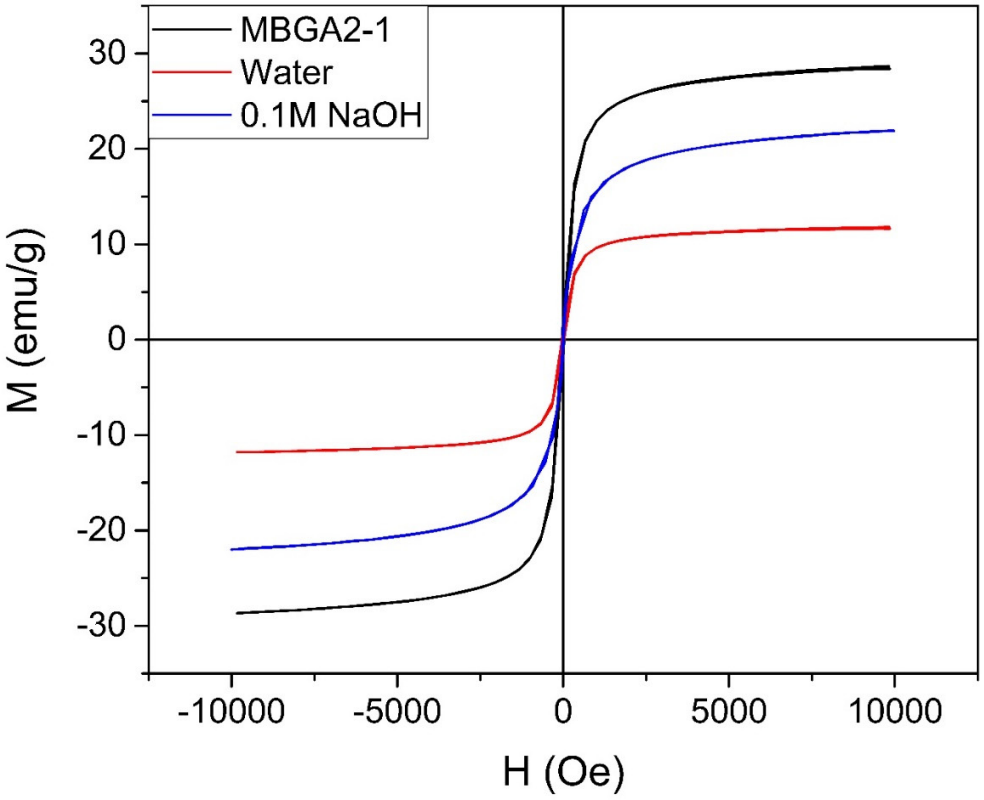

Figure S11. VSM hysteresis loop of (black) fresh MBGA2-1, and MBGA2-1 after used 4 cycles by using (red) water and (blue) 0.1M NaOH as eluents.

Table S1. The elemental compositions obtained from EDX spectra

Samples	%C	SD	%O	SD	%Fe	SD	%Si	SD	%Ca	SD	Other	SD
BGA	60.10	15.67	24.40	9.36	1.27	0.90	7.43	4.47	1.53	0.84	5.33	1.31
MBGA2-0.5	58.87	9.95	27.13	4.14	8.97	5.22	2.70	0.36	0.63	0.21	1.73	0.25
MBGA2-1	24.67	7.98	26.13	9.84	40.27	4.16	3.83	1.50	0.90	0.10	4.17	1.43
MBGA2-2	18.93	8.93	29.50	13.70	45.50	20.94	2.83	1.45	0.33	0.31	2.93	1.16

Table S2. Assignment of the peaks in FTIR spectra for all samples

Wave no.(cm^{-1})	Assignment	Structures
3600-3000	Stretching O-H	Hydroxyl, Carboxylic acid
3000-2800	Stretching C-H	Aliphatic, olefinic and aromatic hydrocarbons
1700-1500	Stretching C=C or C=O	Olefinic, aromatic hydrocarbons, carbonyl
1130-1000	Stretching Si-O-Si	Silicon oxide
820-710	Stretching Si-C	Silicon carbide
650-550	Stretching Fe-O	Iron Oxide
500-420	Bending Si-O-Si	Silicon oxide

Table S3. Assignment of the peaks in XPS results (C 1s and O 1s) for MBGA2-1

Peak	MBGA2-1	%Area	Peak	Used MBGA2-1	%Area	Peak
	BE (eV)			BE (eV)		
C1s	284.53	38.2	Graphitic C	284.93	52	Graphitic C
	285.52	24.6	sp^3 C	286.53	26.1	C-O
	286.73	26.1	C-O	287.5	14.3	C=O
	288.61	11.1	O-C=O	288.87	7.6	O-C=O
O1s	529.96	17.2	Fe-O	530.32	23.1	Fe-O
	530.95	23.7	C=O	531.2	25.7	C-OH/C-O-C
	531.89	27.3	C-OH/C-O-C	532.12	30.5	C=O
	532.85	21.5	SiO_2	533.2	17.1	SiO_2
	534.02	10.4	C-O	534.37	3.6	C-O

Table S4. The elemental compositions (in wt%) for all samples, as obtained from XPS results**.**

Samples	%C	%O	%Fe	%Si	%Ca	%Mg	%K	%Na	%S	%F	%N
BGA	37.13	35.82	0.82	17.42	3.57	2.32	2.93	-	-	-	-
Fe_3O_4	6.78	26.30	64.54	-	-	-	-	2.39	-	-	-
MBGA2-0.5	11.11	35.76	35.61	13.26	2.20	-	-	2.05	-	-	-
MBGA2-1	13.71	34.40	39.06	8.73	0.53	-	-	3.58	-	-	-
MBGA2-2	12.64	27.94	48.91	7.07	-	-	-	3.38	-	-	-
Used MBGA2-1	25.13	33.85	32.73	4.85	1.71	-	-	-	-	-	1.73
MBGA1-1	15.68	33.06	37.57	10.23	-	-	-	-	3.45	-	-
MBGA5-1	14.52	28.95	45.14	7.52	1.60	-	-	1.93	-	0.34	-

Table S5. Fitted parameters in the Langmuir-Hinshelwood model

Sample	Langmuir-Hinshelwood model parameters	
	k (mg/L·s)	**K_{ads} (L/mg)**
MBGA2-1	836.7224089	0.00066592

Table S6. Literature curated data on the catalyst for TC removal and results from the current studies.

Catalyst	Preparation Method	BET (m^2/g)	M_s (emu/g)	pH	H_2O_2 conc. (mM)	H_2O_2 amount (mmol)	Catalyst loading (g/L)	T (°C)	C_0 (mg/L)	Estimated Fe loading (g/L)	V (mL)	Reaction	Reaction time (min)	%Removal	Q_e(mg/g)	k_1 (min^{-1})	%TOC Removal	Ref.
$MnFe_2O_4$/bio-char composite	Co-precipitation method	121.45	11.75	5.5	100	10	0.5	20	40	-	100	Photo-Fenton Degradation	120	95	76.00	-	37.5	(Lai et al., 2019)
C−TiO_2 nanocomposites	Calcination and acid etching	165.5	-	-	-	-	0.2	-	10	-	50	Photocatalytic Degradation	160	90.8	45.40	0.01258	-	(Ma et al., 2019)
Fe_3O_4@MSC	Co-precipitation and calcination	120.09	28.71	7	10	2.5	0.5	23	50	0.146	250	UV-Fenton Degradation	40	99.2	99.20	-	72.1	(Yu et al., 2019)
Fe_3O_4@void@TiO_2sphere	Sol-gel, calcination, and etching method	101	28.71	7	377	15.08	0.25	RT	40	-	40	UV-Fenton-like Degradation	10	94	150.40	0.51000	26.9	(Du et al., 2017)
Fe/N−C composite	Pyrolysis at 900 °C for 2 h	-	62	7	60	1.5	0.2	-	100	-	25	Ultrasound-assisted Fenton-like Degradation	80	92.77	463.85	-	40	(Yang et al., 2018)
Schorl	-	-	-	3	9.9	0.99	10	40	100	-	100	Fenton-like Degradation	600	95.2	9.52	0.00700	29.8	(Zhang et al., 2018)
Fe_3O_4 nanospheres	Solvothermal at 200 °C for 10 h	25.4	66.8	7	50	1.5	0.5	25	40	116.36	30	Fenton-like Degradation	110	82	65.60	0.01767	32.9	(Nie et al., 2020)
NZVI/g-C_3N_4@EGC composite	Calcination and KBH_4 reduction method	48.41	26.5	5	-	-	0.5	30	30	0.192	60	Photo-Fenton Degradation	120	99.5	59.70	0.02690	-	(Wang et al., 2019)
Fe-MOFs	Solvothermal at 110 °C for 20 h	180.41	-	4.1	98	9.8	0.1	14	50	-	100	Photo-Fenton Degradation	20	82.52	412.60	0.07000	48	(Wu et al., 2020)
Pal@Fe_3O_4	Co-precipitation method	69.4	44.11	7	100	10	0.2	30	100	1.23	100	Fenton-like Degradation	60	72.9	364.50	0.01654	-	(Lian et al., 2019)
Fe_3O_4-Cs	solvothermal at 200 °C for 24 h	20.57	*	3	10	2	0.5	40	48	0.109	200	Fenton-like Degradation	120	96	92.16	0.12700	68.3	(Li et al., 2020)
SCH/GO nanocomposites	Oxidation-co-precipitation method	208.6	-	3.5	1	0.2	0.25	25	15	0.125	200	Photo-Fenton-like Degradation	60	98.3	58.98	0.07746	27.3	(Ma et al., 2020)
yolk-shell $ZnFe_2O_4$	Hydrothermal method 180°C for 6 h	83.1	*	2	20	2	0.3	25	60	0.152	100	Photo-Fenton-like Degradation	40	94.2	188.40	0.07000	-	(Xiang et al., 2020)
Fe/S-doped aerogel	Sol-gel and carbonization method	222	-	6	15	0.3	1	25	10	0.342	20	Fenton Degradation	180	99.56	9.96	-	45	(Wang et al., 2020)
$FeNi_3$@SiO_2	Co-precipitation method	481.58	69.69	7	4.4	0.88	0.5	20	20	-	200	Fenton-like Degradation	180	87	34.80	0.00480	-	(Khodadadi et al., 2019)
MBGA catalyst	Co-precipitation method	96	28.71	3.2	5	0.25	1	28	800	0.4	50	Fenton Degradation	720	90.43	721.32	0.00170	56.7	This work

* means that the catalyst was magnetic, but the author does not have the values of saturation magnetization.